Developmental Cell, Volume *23*

Supplemental Information

MOZ Regulates the *Tbx1* Locus, and *Moz* Mutation Partially Phenocopies DiGeorge Syndrome

Anne K. Voss, Hannah K. Vanyai, Caitlin Collin, Mathew P. Dixon, Tamara S. McLennan, Bilal N. Sheikh, Peter Scambler, and Tim Thomas

Inventory of Supplemental Information

Supplemental data

Figure S1, related to Figure 1: Craniofacial, palate, aortic arch and cardiac abnormalities in *Moz* mutant neonates and embryos.

Figure S2, related to Figure 3: Expression of *T-box* genes in $\mathit{Moz}^{\Delta/\Delta}$ embryos.

Figure S3, related to Figure 6: Rescue of the $\mathit{Moz}^{\Delta/\Delta}$ mutant cardiac septal defect by a *Tbx1* transgene – serial images of $\mathit{Moz}^{\Delta/\Delta}$ mutant and *Tbx1* transgenic $\mathit{Moz}^{\Delta/\Delta}$ mutant hearts.

Supplemental Experimental Procedures

Table, related to Experimental Procedures: cDNA templates for cDNA and cRNA probes.

Table, related to Experimental Procedures: Primers used for RT-qPCR experiments.

Table, related to Experimental Procedures: Primers used for qPCR in ChIP experiments

Supplemental References

Supplemental data

Voss_Fig S1

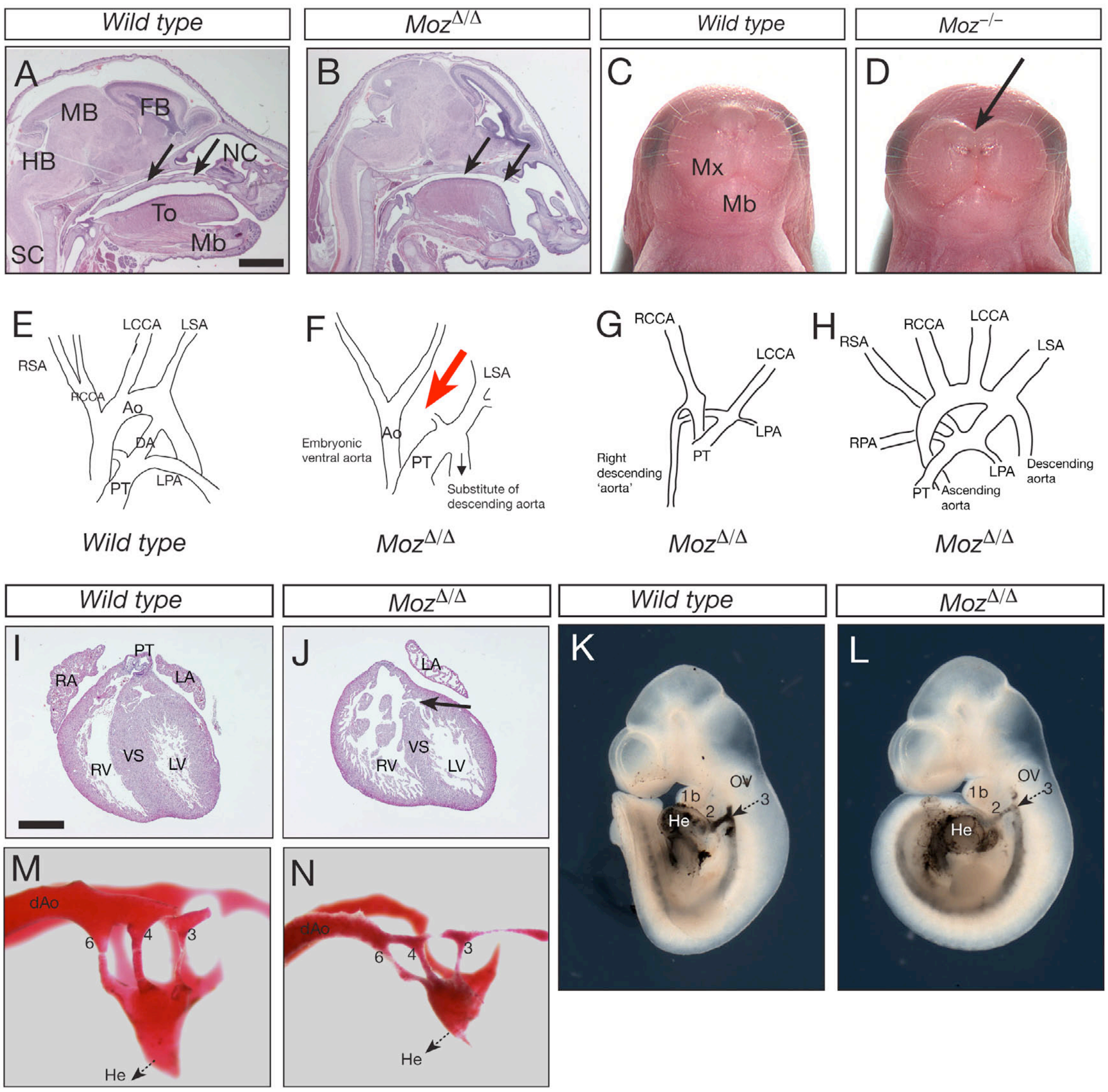

Figure S1: Craniofacial, palate, aortic arch and cardiac abnormalities in *Moz* mutant neonates and embryos. E18.5 *Moz*$^{+/+}$ (A, C), *Moz*$^{\Delta/\Delta}$ (B) and *Moz*$^{-/-}$ (D). (A, B) Sagittal, H&E stained section and (C, D) frontal view of the head. Note the absence of the palate (arrows B vs. A) and incomplete midline fusion of the face (arrow in D vs. C).

(E-H) Schematic drawing of the aortic arch defects in *Moz*$^{\Delta/\Delta}$ mutant pups at E18.5. (E) Wild type vs. (F) the most common abnormality, interrupted aortic arch type B, which occurred in 14 of 19 *Moz*$^{\Delta/\Delta}$ mutant pups examined. Among these, three had an abnormal right descending aorta as depicted in (G). The remaining 5 of 19 pups had less severe abnormalities with abnormal origin of the RSA, abnormally large diameters and lack of wall structure development in the large blood vessels as seen in (H). None of 28 *Moz*$^{\Delta/+}$ heterozygous and wild type, littermate control pups exhibited abnormalities of the aortic arch.

(I-N) The cardiovascular defects in *Moz*$^{\Delta/\Delta}$ mutant pups. E18.5 *Moz*$^{+/+}$ (I) and *Moz*$^{\Delta/\Delta}$ (J) H&E stained transverse sections of hearts. Compared to Fig. 1N,O, note the milder ventricular septal defect (arrow in J vs. I). (K, L) Overview of ink-injected large vasculature of E9.5 *Moz*$^{+/+}$ (K) and *Moz*$^{\Delta/\Delta}$ (L), which appear similar at E9.5 as opposed to the differences seen at E10.5 (Fig. 1). (M, N) Right lateral view of resin-injected large vasculature of E10.5 *Moz*$^{+/+}$ (M) and *Moz*$^{\Delta/\Delta}$ (N). Note that, in contrast to the absence of the 4th pharyngeal arch artery on the left body side in the *Moz*$^{\Delta/\Delta}$ mutants (Fig. 1), the 4th pharyngeal arch artery is present on the right body side *Moz*$^{\Delta/\Delta}$ (N), albeit thinner than in the wild type control (M).

1b, mandibular portion of the 1st pharyngeal arch; 2, 2nd pharyngeal arch; 3, 4, 6, 3rd, 4th and 6th pharyngeal arch artery; Ao; aorta; dAo, dorsal aorta; DA, ductus arteriosus; FB, forebrain; He, heart; HB, hindbrain; LA, left atrium; LCCA, left common carotid artery; LSA, left subclavian artery; LPA, left pulmonary artery; LV, left ventricle; Mx, maxilla; Mb, mandible; MB, midbrain; NC, nasal cavity; OV, otic vesicle; PT, pulmonary trunk; RA, right atrium; RCCA, right common carotid artery; RSA, right subclavian artery; RV, right ventricle; SC, spinal cord; To, tongue; VS, ventricular septum. Scale bar equals 1340 µm in (A, B), 2.8 mm in (C, D), 590 µm in (I, J), 1300 µm in (K, L) and 180 µm in (M, N).

Voss_Fig S2

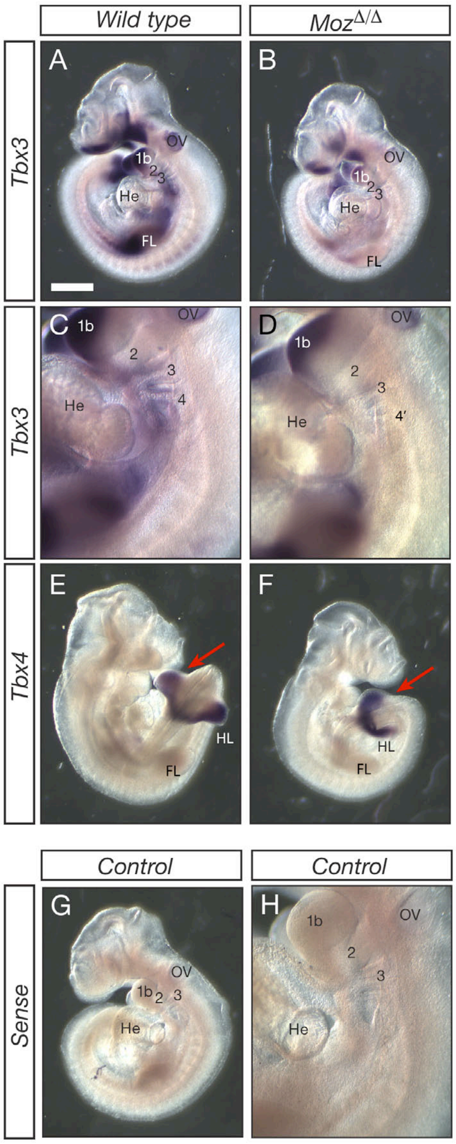

Figure S2: Expression of *T-box* genes in *Moz*$^{\Delta/\Delta}$ embryos. E10.5 *Moz*$^{+/+}$ (A, C, E) and *Moz*$^{\Delta/\Delta}$ (B, D, F) embryos. Whole-mount *in situ* hybridization for expression of *Tbx3* (A-D), *Tbx4* (E, F), and *sense* control in control embryos (G, H). Note the reduction in *Tbx3* mRNA signal (dark purple; A vs. B, C vs. D). In contrast, *Tbx4* mRNA signal is not reduced in the *Moz*$^{\Delta/\Delta}$ embryos (arrows in E, F). 1b, mandibular aspect of the 1st pharyngeal arch; 2, 3, 4, 2nd, 3rd and 4th pharyngeal arch; 4', region where the 4th pharyngeal arch should be present in the *Moz*$^{\Delta/\Delta}$; FL, forelimb bud; He, Heart; HL, hindlimb bud; OV, otic vesicle. Scale bar equals 1700 µm in (A, B), 470 µm in (C, D, G), 1860 µm in (E, F), 1480 µm (H).

Voss_Fig S3

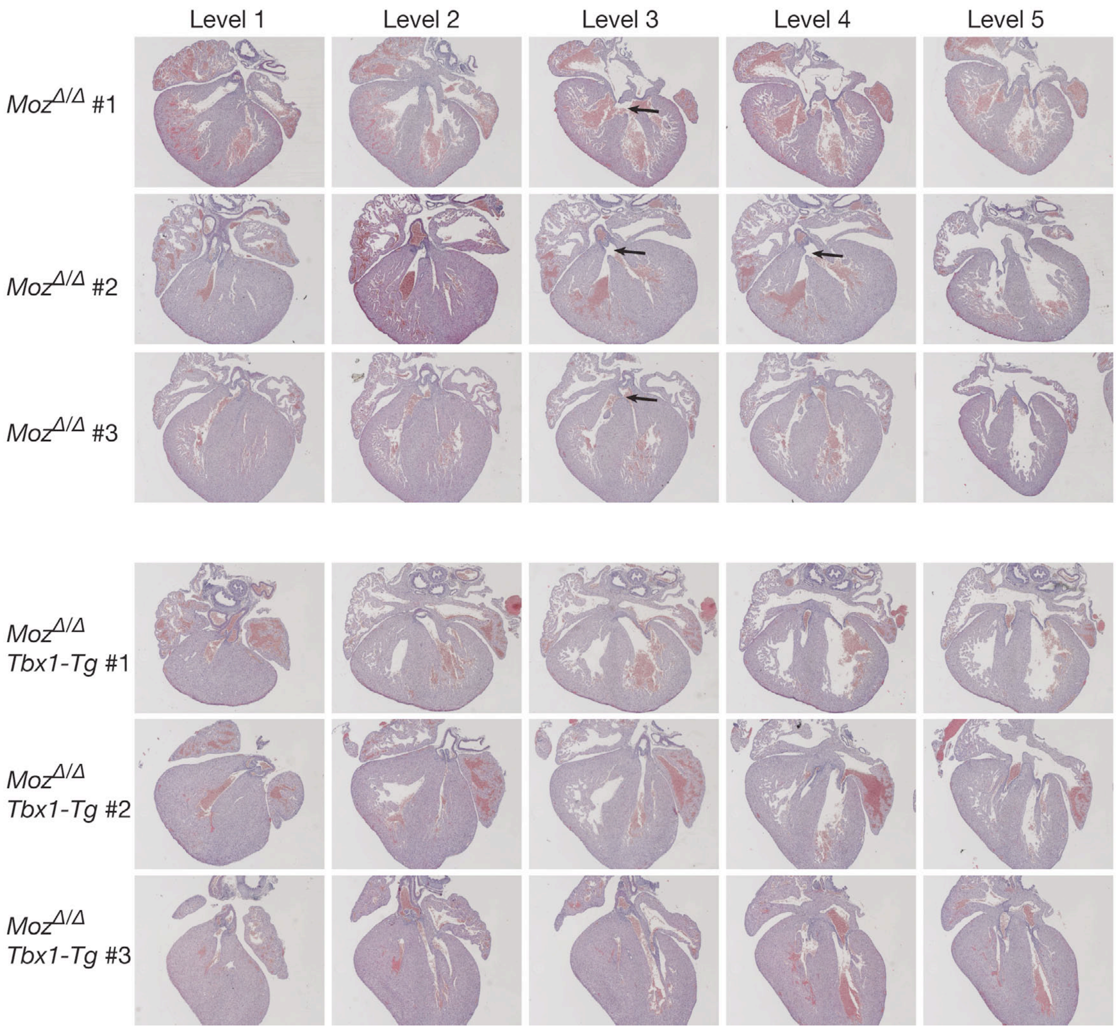

Figure S3: Rescue of the *Moz*$^{\Delta/\Delta}$ mutant cardiac septal defect by a *Tbx1* transgene – serial images of *Moz*$^{\Delta/\Delta}$ mutant and *Tbx1* transgenic *Moz*$^{\Delta/\Delta}$ mutant hearts. Images of haematoxylin and eosin stained paraffin serial sections of three E18.5 *Moz*$^{\Delta/\Delta}$ and three *Moz*$^{\Delta/\Delta}$ *Tbx1-Tg* hearts at five ventro-dorsal levels. Note the large, medium and small ventricular septal defects in the *Moz*$^{\Delta/\Delta}$ mutant hearts (arrows) and the absence of ventricular septal defects in the *Moz*$^{\Delta/\Delta}$ *Tbx1-Tg* hearts. The penetrance of ventricular septal defects in the *Moz*$^{\Delta/\Delta}$ mutants is 95% (Table 1).

Supplemental Experimental Procedures

cDNA templates for cDNA and cRNA probes.

Gene	Provided by	Ref.
Tbx1	V. E. Papaiaonnou	(Chapman et al., 1996)
Tbx2	V. E. Papaiaonnou	(Chapman et al., 1996)
Tbx3	V. E. Papaiaonnou	(Chapman et al., 1996)
Tbx4	V. E. Papaiaonnou	(Chapman et al., 1996)
Tbx5	V. E. Papaiaonnou	(Chapman et al., 1996)
Hsp90β		(Voss et al., 2000)

Primers used for RT-qPCR experiments.

Gene	GeneBank accession number	Forward	Reverse	Correspond-ing to exons*
Tbx1	NM_011532	GTGGACCCTCGAAAAGACAG	CCTACCAGAATCACCGGATC	4-5
Tbx2	NM_009324	AGATGGTCATCACCAAGTCC	CGATGTCCATTAGCAGGATG	1-2
Tbx5	NM_011537	ACACATCGTGAAAGCAGACG	TAACTCCAGGTCATCACTGC	6-7
Tbx20	NM_00120505	AGCTCTCCTCTCGAGCCAAT	GCACATGATGATTTCTCCACAA	1-2
Chd7	NM_0010814417	GGAGAACCCTGAGTTTGCTG	ACCACAGGTCCAGTGAGGAG	Exons 37-38
Foxa2	NM_010446	GAGCCGTGAAGATGGAAGG	CATGTTGCTCACGGAAGAGTAG	Exons 2-3
Foxc1	NM_008592	GCCAGAGCTCCCTCTACAGC	CTGCAGGTTGCAGTGGTAAG	Exon 1
Foxc2	NM_013519	CATGCAGGCGCGTTACTC	CCGCCCGGTAGTAGTTTTG	Exon 1
Gata4	NM_008092	CTGGAAGACACCCCAATCTC	GTAGTGTCCCGTCCCATCTC	Exons 1-2
Gnb1l	NM_001081682	GCTCTGCTGGGAAGGTACTG	GCAATTCCAGGATTGGTGAG	Exons 7-8
Gp1bb	NM_001001999	CGCCTCTCCAGAACGAAGTA	GCTAGCAACAGAAGCAGCAG	Exon 1
Nkx2-5	NM_008700	TTGGCGTCGGGGACTTGAAC	AGGCTACGTCAATAAAGTGG	Exon 4
Pgk1	NM_008828	TACCTGCTGGCTGGATGG	CACAGCCTCGGCATATTTCT	Exons 8–9
Pitx2	NM_011098	GCTACCCAGACATGTCCACTC	AAGCCATTCTTGCACAGCTC	Exons 4-5
Rpl13a	NM_009438	GGAGAAACGGAAGGAAAAGG	TGAGGACCTCTGTGAACTTGC	Exons 7–8
Hsp90ab1	NM_008302	AGAATCCGACACCAAACTGC	ACCTGGGAACCATTGCTAAG	Exon 10

*PCR primers were intron flanking where possible.

Primers used for qPCR in ChIP experiments

Gene	Tile	Forward	Reverse	Size [bp]	Starts at bp from exon 1
Tbx1	*_1*	GTCCGCGTCTATACTGTCAGG	TTTCTTCCTGTCCCAGAGTCC	128	-1005
Tbx1	*_2*	TTTACGATTGAAAGGGCAAAG	TTTCTCGGTGTCACTCTCTCC	114	-490
Tbx1	*_cds*	ATGCTTTCCATAGCTCCTCCTG	GCTTGTCGAAAGACACAATCTG	132	exon 3
Tbx2	*_1*	GGAAGAGATAGATGGGCTTGC	GTGAGCGCACCTTCTACAGAG	130	-807
Tbx2	*_2*	TTTTCTTACTGCTGAGGCTTCC	CCTTGATTGCTGATTTTACGC	132	+9
Tbx5	*_1*	GCAGACTTCAGAGAGGCTAAGG	CTCCTCAAGACACACACTGGAG	132	-769
Tbx5	*_2*	TCTTTCCTTCCTTCCTTCCTTC	TTCCACTTCCCATCCTCTTTAC	135	-282
Tbx1	*Forkhead response element*	TCAGCACAGCCAGCCGCTTT	ATTTCCTTTGGCCCCGCCCC	111	- 14728*
Foxc1	*TSS*	ATTGGCTGCCGCCTCCGTAGT	GAGCATCCGTCACCCAGGCGAG		
Foxc2	*TSS*	GGGCGCGGCCTGAAGAAAGTA	GCGGCCGAGCCCGGAAAAA	104	- 49
Pitx2	*TSS*	CCGCCGCAGAGTGACGTCTTG	CCCCAGCGAGAGACCGGCA	106	- 52
B2m	5' of TSS	TGAACGACCAGATACACCAAAC	AAAGGGACTTTCCCATTTTCAG	128	- 241
Albumin	TSS	GGGGTAGGAACCAATGAAATG	ATTTTGCCAGAGGCTAGTGG	132	-97
Hemoglobin b1	TSS	GTAAGGGCCAATCTGCTCAC	TGTCTGTTTCTGGGGTTGTG	133	-84

*qPCR product encompasses FOXA2/FOXC1/FOXC2 response element as published (Yamagishi et al., 2003).

Supplemental References

Chapman, D.L., Garvey, N., Hancock, S., Alexiou, M., Agulnik, S.I., Gibson-Brown, J.J., Cebra-Thomas, J., Bollag, R.J., Silver, L.M., and Papaioannou, V.E. (1996). Expression of the T-box family genes, Tbx1-Tbx5, during early mouse development. Dev Dyn *206*, 379-390.

Voss, A.K., Thomas, T., and Gruss, P. (2000). Mice lacking HSP90beta fail to develop a placental labyrinth. Development *127*, 1-11.

Yamagishi, H., Maeda, J., Hu, T., McAnally, J., Conway, S.J., Kume, T., Meyers, E.N., Yamagishi, C., and Srivastava, D. (2003). Tbx1 is regulated by tissue-specific forkhead proteins through a common Sonic hedgehog-responsive enhancer. Genes Dev *17*, 269-281.